



Thermal barrier coating toughness: Measurement and identification of a bridging mechanism enabled by segmented microstructure

Erin M. Donohue^{a,*}, Noah R. Philips^a, Matthew R. Begley^{a,b}, Carlos G. Levi^{a,b}

^a Materials Department, University of California, Santa Barbara, United States

^b Mechanical Engineering Department, University of California, Santa Barbara, United States

ARTICLE INFO

Article history:

Received 18 September 2012

Received in revised form

27 November 2012

Accepted 30 November 2012

Available online 8 December 2012

Keywords:

Toughness

Thermal barrier coatings

Yttria-stabilized zirconia

Fracture mechanisms

Crack bridging

ABSTRACT

Failure mechanisms in thermal barrier coatings (TBCs) often involve the propagation of delamination cracks within the top coating. The work presented in this paper makes two principal contributions: first, the development of a straightforward testing geometry and analysis approach enables the accurate determination of the mode I fracture toughness of these coatings and second, the application of the approach to technologically relevant coatings produces new insights into the impact of the dense vertically cracked (DVC) microstructure on the toughness. Mode I toughness of air plasma-sprayed 8 wt% yttria-stabilized zirconia DVC TBCs is measured by sandwiching the freestanding coatings in a modified double cantilever beam configuration. Digital image correlation measurements and finite element analysis provide a pathway to quickly and accurately extract toughness values from displacement data alone. Results show R-curve behavior and unexpectedly high steady-state toughness values of $G_{ss} \approx 300\text{--}400 \text{ J/m}^2$. The observation of this elevated toughness can be rationalized by a crack bridging model that is consistent with the TBC's starting microstructure and features of the fracture surfaces.

© 2012 Elsevier B.V. All rights reserved.

1. Introduction

Thermal barrier coatings (TBCs) are key components of multi-layered thermal protection systems in gas turbines, which enable greater fuel efficiency by allowing operation at increased temperatures [1,2]. The lifetime of a coating is often strongly dependent on its toughness, a property that determines the extent of various failure mechanisms [2], both intrinsic (e.g. thickening or rumpling of the thermally grown oxide [3–7]) and extrinsic (e.g. impact damage [8–11] and cracking due to molten siliceous deposits [12–15]). Hence, predictions of coating durability and design of future TBCs often rely critically on an accurate assessment and understanding of toughness.

While the importance of measuring TBC toughness is clear [10,14], there are relatively few direct measurements on pertinent microstructures [16–18]. (Indirect assessments on the intrinsic toughness of the appropriate composition, 8 wt% yttria-stabilized zirconia (8YSZ), include [19–21]). Coatings examined in this article are produced by air plasma spray (APS) and contain segmented cracks in the thickness direction to provide greater strain tolerance upon thermal cycling (Fig. 1) [22–25]. While standard APS coatings are highly porous to attain low thermal

conductivity, the processing conditions to create the segmented cracks cause the intervening material to have significantly less porosity [26]. Referred to as dense vertically cracked (DVC) microstructures, these coatings can still maintain a sufficiently high thermal gradient in operation [25,26]. In order to probe the behavior of materials used in actual turbines, the difficult task of fabricating suitable fracture specimens from thin, freestanding, ceramic coatings must be overcome.

Here, fracture experiments are conducted using a modified double cantilever beam (DCB) geometry, where the TBC is sandwiched between two steel beams and tested in displacement control via wedge loading (Fig. 2). Quantification of R-curve behavior is possible provided that (i) the crack tip can be correctly determined as a function of the beam deflection and (ii) the energy release rate can be calculated accurately while accounting for complicating factors such as the finite compliance of the ceramic layer and transverse shear effects. These interrelated challenges are addressed by the combination of digital image correlation (DIC) measurements and finite element (FE) analysis.

A key insight in the present approach, which facilitates the extraction of the crack tip location from DIC data, is that the centerline of the beams experiences negative displacements just ahead of the crack tip (Fig. 2). This feature is observed in both the FE results and analytical models of beams on finite-sized elastic foundations (i.e. the length of the TBC in the sandwich). In both analyses, it is revealed that the distance between the onset of the

* Corresponding author. Fax: +1 805 893 8486.

E-mail address: erin_donohue@engineering.ucsb.edu (E.M. Donohue).

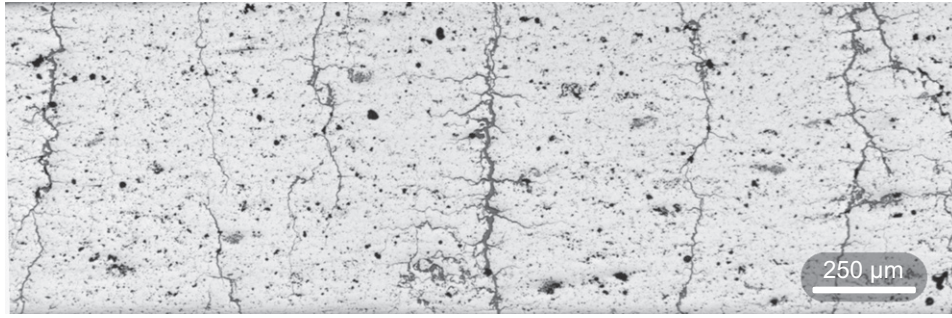


Fig. 1. A cross-sectional view of an 8YSZ APS coating with a segmented microstructure comprising of through-thickness cracks that form an in-plane mud cracking pattern, which define pillar-like features that enable the toughening mechanism discussed herein.

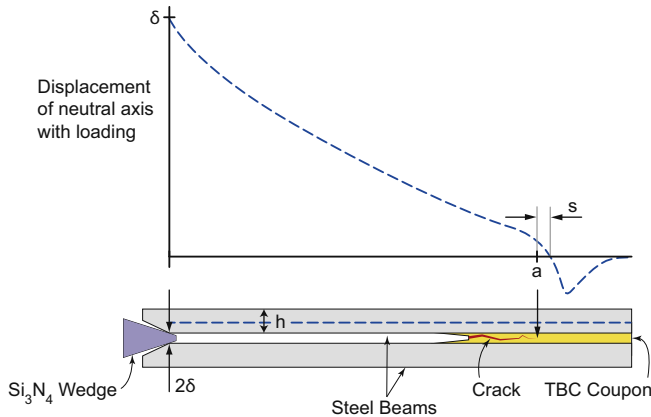


Fig. 2. The DCB configuration (at bottom) and a schematic displacement trace of the mid-line of the steel beam. The offset, s , indicates the location of the crack tip relative to the onset of negative displacement (an effect of the compliant foundation, exaggerated here, see also Fig. 4).

region of negative displacements and the crack tip location is, perhaps surprisingly, insensitive to reasonable variations in specimen dimensions and TBC properties. Thus, a simple method is developed to determine the crack length from DIC displacement measurements using a fitting procedure from FE results.

The toughness measurements elucidated by this approach reveal R-curve behavior with steady-state values that are appreciably higher than the initiation toughness. This result and features observed on the fracture surface strongly suggest that a crack bridging and pull-out mechanism, which develops as a consequence of the DVC microstructure, is responsible for the substantial improvement of the TBC's macroscopic resistance to fracture.

2. Experimental approach

Each DCB specimen was fabricated by sandwiching a TBC between two steel beams. Freestanding APS-DVC coatings (kindly provided by GE Energy), $25.4 \text{ mm} \times 25.4 \text{ mm} \times 1 \text{ mm}$, were impregnated with M-bond 610 epoxy (Vishay Micro-measurements) to minimize damage during sample preparation. A surface grinder with a 400 grit diamond wheel established flat, parallel surfaces. The coatings were subsequently sectioned into beams ($25.4 \text{ mm} \times 6.35 \text{ mm} \times 1 \text{ mm}$) using a diamond blade and the epoxy was removed by oxidative decomposition in air at $700 \text{ }^\circ\text{C}$.

To ensure adequate adhesion, the surfaces of two 304 stainless steel cantilevers ($63.5 \text{ mm} \times 6.35 \text{ mm} \times 3 \text{ mm}$) were first ground and then cleaned with acetone. A rubber-toughened adhesive film (FM-1000 from CYTEC Industries) was used to bond the YSZ to one end of the beams. This high viscosity epoxy exhibited minimal

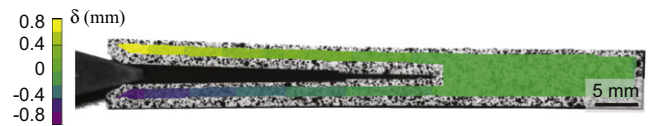


Fig. 3. In situ optical image of a speckled DCB specimen with overlaid displacement contours from digital image correlation measurements.

infiltration into the porous TBC. After curing at $170 \text{ }^\circ\text{C}$, subject to a pressure of 180 kPa, the epoxy was limited to an approximately $60 \text{ } \mu\text{m}$ thick film at the steel/TBC bond line. A small notch, introduced to the TBC using a diamond wafering blade, assisted crack initiation. During the test, the far end of the specimen was supported on a rigid base, with an intervening, soft metallic foil. At the loading end, a Si_3N_4 wedge, with a 15° half angle, was lubricated with graphite (Crown 8078). Samples were tested at room temperature on a servo-hydraulic test frame (MTS 810) under displacement control.

Images of the specimen were captured at 15–20 s intervals so that the displacement of the cantilevers, including at the location of the wedge (δ), could be measured using DIC (Fig. 3). To facilitate displacement mapping, the assembled specimen was speckled with black on white spray paint. After the experiment was completed, the VIC2D DIC software from Correlated Solutions Inc. compared all images to an initial calibration image taken immediately before testing commenced [27]. The area of interest was defined as the entire speckled surface; the subset size was set to 51 pixels (to reduce noise), the step size was 5 pixels, and the magnification was typically $0.028 \pm 0.002 \text{ mm/pixel}$. A series of correlations on unstrained samples established the displacement resolution at better than $1 \text{ } \mu\text{m}$.

3. Calculations

Imaging limitations did not allow for a precise optical determination of the crack tip location and compliance methods were inaccurate for the chosen geometry, resulting in an overestimation of energy release rate. Numerical analysis, through FE simulations in ABAQUS/CAE, facilitated accounting for complex interactions such as the extent of deviations from Bernoulli–Euler beam theory (for one, shear effects at the crack tip) and the presence of the compliant foundation [28–30]. As such, a 2D FE model was utilized to provide values of energy release rate for a set of geometric (lengths: L_{steel} , L_{TBC} and thicknesses: h_{steel} , h_{TBC}) and elastic (E_{steel} , E_{TBC}^1) parameters, a given crack length (a), and opening displacement at the load point (δ).

¹ E_{TBC} is actually an effective modulus that combines the contributions of the TBC and the epoxy.

Download English Version:

<https://daneshyari.com/en/article/7983401>

Download Persian Version:

<https://daneshyari.com/article/7983401>

[Daneshyari.com](https://daneshyari.com)